Analysis and design of a DC voltage-controlled static VAr compensator using quad-series voltage-source inverters

Hideki Fujita
Okayama University

Shinji Tominaga
Okayama University

Hirofumi Akagi
Okayama University

Analysis and Design of a DC Voltage-Controlled Static Var Compensator Using Quad-Series Voltage-Source Inverters

Hideaki Fujita, *Member, IEEE*, Shinji Tominaga, and Hirofumi Akagi, *Fellow, IEEE*

Abstract—This paper presents a dc voltage-controlled static var compensator (SVC) using quad-series voltage-source non-PWM inverters. The SVC consists of four three-phase voltage-source inverters having a common dc capacitor and four three-phase transformers, the primary windings of which are connected in series with each other. Although each inverter outputs a square wave voltage, the synthesized ac voltage of the SVC has a 24-step waveshape. This results not only in a great reduction of harmonic currents and dc voltage ripples but also in less switching and snubbing losses.

This paper develops the analysis of the transient response and the resonance between the ac reactors and the dc capacitor, with the focus on practical use. Experimental results obtained from a 10-kVA laboratory system are shown to agree well with the analytical results, thus verifying the analysis and leading to the design of dc capacitance value.

I. INTRODUCTION

STATIC var compensators (SVC's) rated at $50 \sim 300$ Mvar, consisting of voltage source inverters using gate-turn-off (GTO) thyristors, are showing promise of improving power factor and stabilizing transmission systems. The SVC's can adjust the amplitude of the ac voltage of the inverters by means of pulse-width modulation (PWM) or by controlling the dc bus voltage, thus producing either leading or lagging reactive power [1]–[8].

A pulse-width-modulated SVC [1]–[5], in which the dc voltage is controlled to remain at a constant value, can respond rapidly to a change in reactive power at the expense of increasing the switching and snubbing losses. High efficiency and high reliability are a priority in practical power system applications of the SVC's.

On the other hand, a dc voltage-controlled SVC [6]–[8], which directly controls the dc capacitor voltage by causing a small amount of active power to flow into or out of the voltage-source inverters, results in less switching and snubbing losses because the switching frequency is low. However, it has been pointed out that the dc voltage-controlled SVC is inferior to the PWM SVC in the transient response of reactive

power. Some papers and articles dealing with the dc voltage-controlled SVC have been published, but they have excluded analysis of the transient response of reactive power and have assumed a constant dc bus voltage. Based on this, they have provided the following interpretations:

- The smaller the capacitance, the faster the response of reactive power.
- The larger the capacitance, the smaller the voltage fluctuation across the dc capacitor.

In this paper, an analysis of the dc voltage-controlled SVC consisting of quad-series voltage-source non-PWM inverters is presented, and includes the transient response of reactive power along with the design of the dc capacitor. A model for the SVC based on the pq theory [1] is developed, and has the ability to deal with the power flow between the ac and dc sides in a transient state. This analysis leads to the following results which cannot be explained by the conventional interpretations mentioned above:

- The capacitance value of the dc capacitor has almost no effect on the transient response of reactive power.
- The dc voltage fluctuation is not in inverse proportion to the capacitance value.
- The SVC falls into resonance between the dc capacitor and the ac reactors at a specified frequency.

Some experimental results obtained from a 10 kVA laboratory system agree well with the analytical results. Moreover, it is shown by experiment and analysis that a feedback control loop of instantaneous reactive power makes it possible to achieve a 5-ms step response time of reactive power.

II. DC VOLTAGE-CONTROLLED SVC

A. Experimental System Configuration

Fig. 1 shows the system configuration of a 10 kVA static var compensator consisting of quad-series voltage-source inverters. The circuit parameters are shown in Table I. Each three-phase inverter is characterized by an ac line-to-line voltage having a six-step waveform. The dc links of the four voltage-source inverters are connected in parallel with a common dc capacitor of 500 μF. The ac terminals of the inverters are connected to the supply via four three-phase transformers, the detailed configuration of which is shown in Fig. 2. Each transformer has three-phase windings of Δ or Y connection in the primary, which are separated phase by phase,
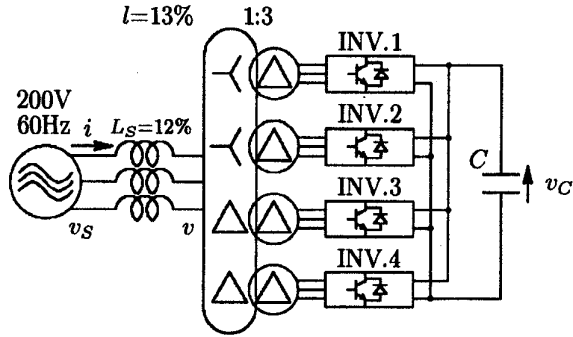
Fig. 1. Experimental system configuration.

TABLE I
CIRCUIT PARAMETERS OF EXPERIMENTAL SYSTEM

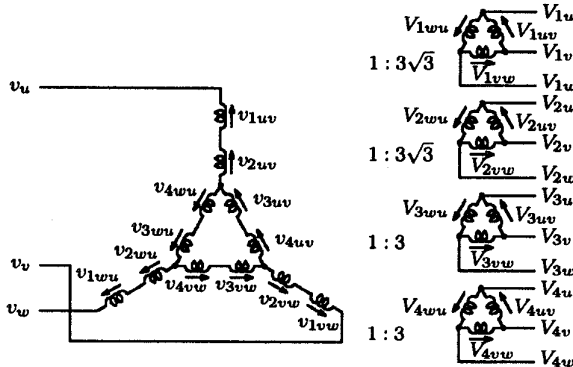| reactive power rating	Q	10kVA
line to line supply voltage	V_S	200V
angular supply frequency	ω_0	$2\pi \times 60$rad/s
dc voltage	V_C	150~230V
capacitance of dc capacitor	C	500μF
inductance of ac reactors	L_S	1.3mH(12%)
leakage inductance	l	1.4mH(13%)
equivalent inductance	$L(= L_S + l)$	2.7mH(25%)
equivalent resistance	R	0.28Ω
ac to dc voltage ratio	K	1.03
unit capacitance constant	UCC	1.3×10^{-3}J/VA

Fig. 2. Connection of four three-phase transformers.

and has Δ-connected three-phase windings in the secondary. The primary to secondary voltage ratio for each transformer is 1 : 3.

In Fig. 1, the inverters INV.1 and INV.3 operate at a leading phase-angle of 7.5° with respect to the supply voltage, while INV.2 and INV.4 operate at a lagging phase-angle of 7.5°. This results in a great reduction of supply harmonic currents and dc link voltage ripples because the synthesized ac voltage of the SVC looks like a 24-step waveform. The fundamental component of the synthesized voltage is given by

$$V = \frac{\sqrt{6}}{\pi} mnV_C \cos \frac{\pi}{24} \quad (1)$$

where m is the number of the series connected inverters, and n is the primary-to-secondary voltage ratio for each transformer. Since $m = 4$ and $n = 1/3$ in the experimental system, the
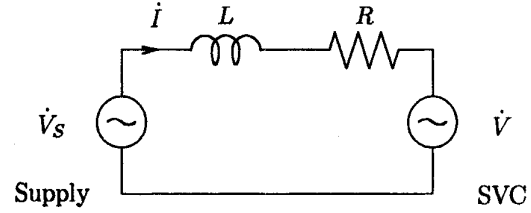

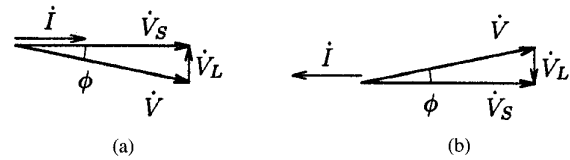Fig. 3. Single-phase equivalent circuit.

Fig. 4. Phaser diagram of the SVC.

ratio K is 1.03, representing the fundamental component of the synthesized ac voltage with respect to the dc voltage of the SVC.

B. Unit Capacitance Constant

A unified constant is introduced to lead to the design of the capacitance of a dc capacitor in an SVC consisting of voltage-source inverters. It is named the "unit capacitance constant (UCC)" in this paper, associated with the unit inertia constant in synchronous rotary condensers. In the experimental system, it is given by

$$\text{UCC} = \frac{1}{2}CV_C^2/Q = 1.3 \times 10^{-3}[\text{J/VA}]$$

where $C = 500$ μF, $V_C = 230$ V and $Q = 10$ kVA.

C. Basic Principle in Steady State

Fig. 3 shows a single-phase equivalent circuit of the SVC, where $\dot{V}_S$ is the supply voltage phaser, $\dot{V}$ is the ac voltage phaser of the SVC, and $L(= L_S + l)$ and R represent the equivalent inductance and resistance of the SVC. The reactive power of the SVC can be adjusted by controlling the amplitude of $\dot{V}$. If $|\dot{V}_S| > |\dot{V}|$, the SVC draws a lagging reactive power from the supply, acting as a reactor, while, if $|\dot{V}_S| < |\dot{V}|$, it draws a leading one, acting as a capacitor. The dc voltage-controlled SVC can control the amplitude of the ac voltage by causing a small amount of active power to flow into or out of the SVC.

Fig. 4(a) shows a phaser diagram in the case that $\dot{V}$ lags $\dot{V}_S$. Here, ϕ is the phase angle of $\dot{V}$ with respect to $\dot{V}_S$, and $\dot{I}$ is a supply current phaser. In Fig. 4(a), $\dot{I}$ is in phase with $\dot{V}_S$, so that a small amount of active power flows into the SVC, thus the dc capacitor is charged. In the case where $\dot{V}$ leads $\dot{V}_S$, as shown in Fig. 4(b), a small amount of active power flows out, thus the dc capacitor is discharged. Accordingly, a large amount of reactive power drawn by the SVC can be controlled by adjusting the phase angle ϕ by a small amount.

III. TRANSIENT ANALYSIS FOR SVC

A. Modeling of SVC

For the sake of simplicity, the following assumptions are made in modeling the SVC:

1) Any harmonic voltage caused by the switching operation of the inverters is excluded from the synthesized ac voltage of the SVC.
2) The instantaneous amplitude of the fundamental component of the ac voltage is proportional to the instantaneous voltage of the dc capacitor.
3) No power loss occurs in the inverters; therefore the active power on the ac side is equal to the active power on the dc side.

Assumptions 1 and 2 mean that the harmonic voltage caused by fluctuation of the dc voltage is included in the synthesized ac voltage.

Assume an ideal three-phase power supply given by

$$
\begin{bmatrix} v_{Su} \\ v_{Sv} \\ v_{Sw} \end{bmatrix} = \sqrt{\frac{2}{3}} V_S \begin{bmatrix} \cos \omega_0 t \\ \cos(\omega_0 t - 2\pi/3) \\ \cos(\omega_0 t + 2\pi/3) \end{bmatrix} \tag{2}
$$

where V_S is the rms voltage of the supply and ω_0 is its angular frequency. Assumptions 1 and 2 lead to the following ac voltage of the SVC:

$$
\begin{bmatrix} v_u \\ v_v \\ v_w \end{bmatrix} = \sqrt{\frac{2}{3}} K v_C \begin{bmatrix} \cos(\omega_0 t + \phi) \\ \cos(\omega_0 t - 2\pi/3 + \phi) \\ \cos(\omega_0 t + 2\pi/3 + \phi) \end{bmatrix} \tag{3}
$$

where ϕ is the angle of the fundamental ac voltage with respect to the supply voltage, and K is the ac to dc voltage ratio of the SVC. Using Fig. 3, one obtains the following equation:

$$
\begin{bmatrix} v_{Su} \\ v_{Sv} \\ v_{Sw} \end{bmatrix} = \left(R + L \frac{d}{dt} \right) \begin{bmatrix} i_u \\ i_v \\ i_w \end{bmatrix} + \begin{bmatrix} v_u \\ v_v \\ v_w \end{bmatrix}. \tag{4}
$$

Invoking Assumption 3 results in the following equation for active power:

$$
p = v_u i_u + v_v i_v + v_w i_w = \frac{d}{dt} \frac{C}{2} v_C^2 = C v_C \frac{dv_C}{dt}. \tag{5}
$$

The pq theory [1] can be used to transform (2)~(5) to

$$
\begin{bmatrix} L\frac{d}{dt} + R & -\omega_0 L \\ \omega_0 L & L\frac{d}{dt} + R \end{bmatrix} \begin{bmatrix} i_p \\ i_q \end{bmatrix} = \begin{bmatrix} V_S - K v_C \cos \phi \\ -K v_C \sin \phi \end{bmatrix}. \tag{6}
$$

Equation (5) can be represented as a function of i_p and i_q as follows.

$$
\frac{dv_C}{dt} = \frac{K}{C} (i_p \cos \phi + i_q \sin \phi). \tag{7}
$$

In (6) and (7), i_p is an instantaneous active current and i_q is an instantaneous reactive current. The instantaneous reactive power drawn from the supply, q_S is given by

$$
q_S = v_{Sp} \cdot i_q - v_{Sq} \cdot i_p = V_S \cdot i_q. \tag{8}
$$

B. Transient Response of Reactive Power

The transient response of instantaneous reactive power q_S to a step change in the phase angle ϕ is discussed. It is, however, difficult to derive a general solution to an arbitrary change in ϕ because the nonlinear functions, i.e., $\sin \phi$ and $\cos \phi$ are included in (6) and (7). In general, nonlinear equations can be linearized by limiting attention to small perturbations around a reference state.

The following analysis assumes a step change in ϕ from 0 to Φ (i.e., $\phi(t) = \Phi \cdot u(t)$, where $u(t)$ is a unit step function). This allows us to deal with the nonlinear functions as constant values which equal $\sin \Phi$ and $\cos \Phi$, respectively, when $t \geq 0$. Note that a small signal perturbation model is not introduced into the linearization developed in this paper. As a result, this analysis is applicable for a large step change in ϕ.

At first, one has to calculate the initial values of i_p, i_q and v_C at time $t = 0$. Such a relationship that the initial values equal their steady-state values at $\phi = 0$ in (6) and (7) gives us their initial values as $i_p(0) = 0$, $i_q(0) = 0$, and $v_C(0) = V_S/K$. Note that the initial value of v_C is not zero.

The Laplace transformations of (6) are represented as follows:

$$
(sL + R)I_p(s) - \omega_0 L I_q(s) = \frac{V_S}{s} - K \cos \Phi V_C(s) \tag{9}
$$

$$
\omega_0 L I_p(s) + (sL + R)I_q(s) = -K \sin \Phi V_C(s). \tag{10}
$$

Taking into account the initial value of v_C, one obtains the Laplace transformation of (7) as follows:

$$
sV_C(s) - v_C(0) = \frac{K}{C} \{\cos \Phi I_p(s) + \sin \Phi I_q(s)\}. \tag{11}
$$

The Laplace function for the reactive power, $I_q(s)$ is obtained from (9), (10), and (11), as follows:

$$
I_q(s) = \frac{-V_S \left\{ \frac{A_1}{L} s + \left(\frac{RA_1}{L^2} + \frac{\omega_0 A_2}{L} \right) + \frac{K^2 A_3}{L^2 C s} \right\}}{s^3 + 2\frac{R}{L} s^2 + \left(\frac{R^2}{L^2} + \frac{K^2}{LC} + \omega_0^2 \right) s + \frac{K^2 R}{L^2 C}} \tag{12}
$$

where

$$
A_1 = \sin \Phi
$$
$$
A_2 = (1 - \cos \Phi)
$$
$$
A_3 = \sin \Phi \cos \Phi.
$$

The following approximation appropriate for the SVC is applied to (12):

$$
R^2/L^2 + K^2/LC \gg \omega_0^2.
$$

This allows us to derive the following basic equation:

$$
I_q(s) \approx \left(-\frac{B_1}{s} + \frac{B_1 - B_2}{s + R/L} + \frac{sB_2 + B_3}{s^2 + (R/L)s + K^2/LC} \right) V_S \tag{13}
$$

where

$$
B_1 = (\sin \Phi \cos \Phi)/R
$$
$$
B_2 = (1 - \cos \Phi)\omega_0 C/K^2
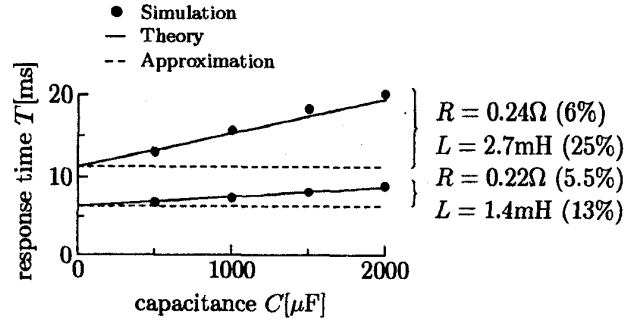$$
$$
B_3 = \sin \Phi(1 - \cos \Phi)/L.
$$

Fig. 5. Relationships between the capacitance value of the dc capacitance and the time constant of response of q_S.

The first and second terms on the right side in (13) are the dominant response of reactive power, while the third term means that an oscillatory component exists. The time constant of the transient response of reactive power, T is equal to the time constant determined by L and R as depicted in Fig. 3 and is given as follows

$$T = \frac{L}{R}. \tag{14}$$

Note that the capacitance of the dc capacitor, C is excluded from (14). This means that the amount of active power flowing into the SVC is proportional to C while the dc bus voltage is rising.

Fig. 5 shows the relationship between the capacity of the dc capacitor and the time constant of the reactive power. The plots for $L (= l) = 1.4$ mH (13%) shown in Fig. 3 represent a practical situation, whereas the plots for $L (= L_S + l) = 2.7$ mH (25%) represent the experimental condition. The equivalent resistor R incorporates the losses of the transformers and the inverters. The solid lines indicate theoretical results without any approximation (see the Appendix), the broken lines indicate the results for (13), and the dots show the results obtained from a detailed simulation.

The simulated results concur with the theoretical results. The theoretical response time shown by the solid lines tends to a small increase as the capacitance of the dc capacitor C is increased. However, the difference in results between the theory and approximation is not so large in the range of capacitances used in the experiment (i.e., $C < 1000$ μF). The approximation is applicable for typical practical systems having a per unit reactance around 15% because the difference becomes small as the equivalent inductance L becomes small.

C. Resonance Between AC Reactors and DC Capacitor

As mentioned above, the third term in (13) is an oscillatory component. In other words, the dc voltage-controlled SVC may exhibit a resonance interaction between the ac reactors and the dc capacitor at a specific frequency. If a harmonic voltage, the frequency of which coincides with such a resonant frequency, were included in the supply, a large amount of harmonic current would flow into the SVC, and an excessive voltage fluctuation would then occur across the dc capacitor.

Assuming a resistance of $R = 0$ in (12), the resonant angular frequency is given by

$$\omega_R = \pm\sqrt{\frac{K^2}{LC} + \omega_0^2}. \tag{15}$$

Since ω_R is the angular frequency on the pq coordinate reference frame or on the dc side of the SVC, the resonance occurs at $\omega_0 \pm \omega_R$ on the ac side of the SVC.

To calculate the fluctuation of the dc voltage and the active power caused by the harmonic voltage in the supply, (6) is expanded as

$$\begin{bmatrix} R + L\frac{d}{dt} & -\omega_0 L \\ \omega_0 L & R + L\frac{d}{dt} \end{bmatrix} \begin{bmatrix} i_p \\ i_q \end{bmatrix} = \begin{bmatrix} v_{Sp} - Kv_C \cos\phi \\ v_{Sq} - Kv_C \sin\phi \end{bmatrix} \tag{16}$$

where v_{Sp} and v_{Sq} are the p and q components of the supply voltage, respectively.

Considering ϕ a constant value in (7) and (16), the Laplace transformed active power component $I_p(s)$ and the dc voltage $V_C(s)$ are given by the following equations:

$$I_p(s) = \frac{1/L}{s^3 + \frac{2R}{L}s^2 + \left(\frac{R^2}{L^2} + \frac{K^2}{LC} + \omega_0^2\right)s + \frac{K^2R}{L^2C}}$$
$$\cdot \left\{ \left(s^2 + \frac{R}{L}s + \frac{K^2\sin^2\phi}{LC}\right)V_{Sp}(s) \right.$$
$$\left. + \left(\omega_0 s + \frac{K^2\sin\phi\cos\phi}{LC}\right)V_{Sq}(s) \right\} \tag{17}$$

$$V_C(s) = \frac{K/LC}{s^3 + \frac{2R}{L}s^2 + \left(\frac{R^2}{L^2} + \frac{K^2}{LC} + \omega_0^2\right)s + \frac{K^2R}{L^2C}}$$
$$\cdot \left[\left\{ \left(s + \frac{R}{L}\right)\cos\phi - \omega_0 \sin\phi \right\} V_{Sp}(s) \right.$$
$$\left. + \left\{ \left(s + \frac{R}{L}\right)\sin\phi + \omega_0 \cos\phi \right\} V_{Sq}(s) \right]. \tag{18}$$

Equation (18) tells us that the amount of dc voltage fluctuation is determined not only by the amplitude of the harmonic voltage included in the supply but also by the operating phase angle ϕ.

Figs. 6 and 7 show the fluctuating components of the dc voltage v_C and that of the active power i_p, respectively, which are caused by a 1% third-order harmonic voltage included in the supply. Here, ϕ is a constant value of -0.06 rad. The third harmonics on the ac side of the SVC make the dc voltage fluctuate at twice the supply frequency. In Fig. 6, the maximum voltage fluctuation, which is 4 V (2% of the dc voltage), appears if $C = 900$ μF because the resonant frequency ω_R for that value of capacitance is equal to twice the supply frequency. At the point of resonance, the amplitude of the harmonic current in i_p reaches 3.5 A, which is 10% of the rated current of the SVC. This resonance could be a serious problem in a practical system, because the equivalent resistance R in a practical system may be smaller than that of the experimental system.

The above analytical results do not agree with predictions in a conventional interpretation. The reason is a conflict between the assumption of dc voltage fluctuation and the calculation of the harmonic current in the supply. That is, the supply harmonic current was calculated under the assumption that no
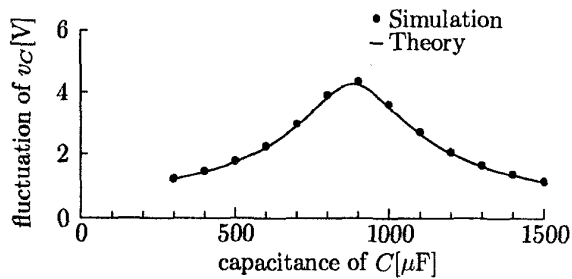
Fig. 6. Voltage fluctuation across the dc capacitor caused by a 1% third harmonic voltage component in the supply voltage.
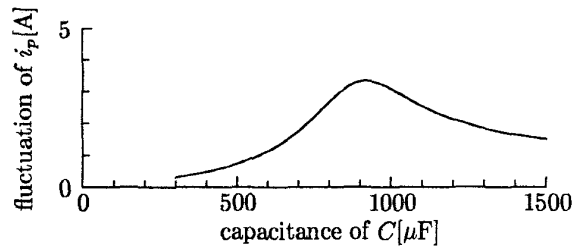

Fig. 7. Harmonic amplitude of i_p caused by a 1% third harmonic voltage component in the supply voltage.

harmonic component is superimposed onto the fundamental component of the ac voltage of the SVC. This means that any dc voltage fluctuation was neglected. But the calculation of the dc voltage fluctuation was performed based on the supply harmonic current calculated under the above assumption of a constant dc bus voltage.

The dc voltage fluctuation affects the supply current I in the model developed in this paper because the ac voltage of the SVC includes the harmonic voltage caused by the dc voltage fluctuation. The resonance between the ac reactors and the dc capacitor occurs, when the harmonic component on the ac side increases the fluctuation of active power flowing into the SVC. The dc voltage fluctuation becomes large as the capacitance value approaches 900 μF as shown in Fig. 6.

IV. CONTROL CIRCUIT

Fig. 8 shows the block diagram of the control circuit. Reactive power feedback using a PI controller makes it possible to improve the transient response of the reactive power. The pq transform circuit calculates the instantaneous reactive power q_S from the three-phase supply voltages v_{Su}, v_{Sv}, and v_{Sw} and the three-phase currents i_u, i_v, and i_w. The calculated reactive power q_S and the reference reactive power q_S^* are applied to the proportional–integral (PI) controller. The output of the PI controller is a reference signal representing the phase angle ϕ^*.

The counter produces the phase information, $\omega_0 t$, from a signal generated by a phase locked loop (PLL) circuit, the frequency of which is $49152 (= 24 \times 2^{11})$ times the supply. The phase comparator compares ϕ with $\omega_0 t$, and determines the time at which the corresponding switching device is turned on or off. The gate control circuit prevents each switching device from being switched on more than once in one cycle due to fast changes in ϕ.
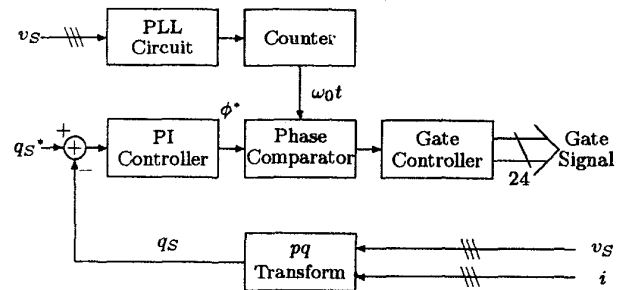

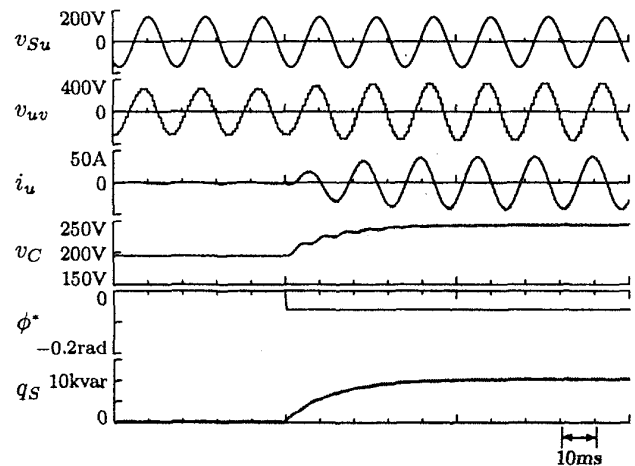Fig. 8. Block diagram of control circuit.

Fig. 9. Simulated waveforms for a step change of ϕ, where $C = 500$ μF.

V. EXPERIMENTAL RESULTS

Figs. 9–12 show simulated and experimental waveforms for a step change of ϕ from 0 to -0.08 rad. The line-to-line voltage of the SVC, v_{uv} has a 24-step wave shape, so that the supply current i_u is almost sinusoidal. Before ϕ is changed, i_u and q_S are equal to zero and the dc link voltage v_C is 190 V. At the instance of the step change, v_C and q_S begin to increase, and finally reach 230 V and 10 kvar, respectively, in 50 ms. The time constant of the transient response in Fig. 10 is almost equal to that in Fig. 12, which is 11 ms, irrespective of the capacity of C. From (14), the theoretical time constant is given by

$$T = \frac{L}{R} = \frac{2.7 \text{ mH}}{0.24 \text{ } \Omega} = 11.2 \text{ ms}$$

which agrees well with the experimental result.

The voltage fluctuation of v_C in Fig. 12 is larger than that in Fig. 10, even if the capacity of C in Fig. 12 is twice the value of C as indicated in Fig. 10. This is due to the resonance between the dc capacitor and the ac reactors (i.e., the resonant frequency in Fig. 12 is twice the supply frequency of 60 Hz). This shows that the reduction of the dc voltage fluctuation can be achieved, not by increasing the capacity of the dc capacitor, but by avoiding the resonance condition.

Figs. 13–16 show experimental waveforms for a step change of the reference reactive power from 0 to 10 kvar, where a reactive power feedback loop, having a feedback gain of
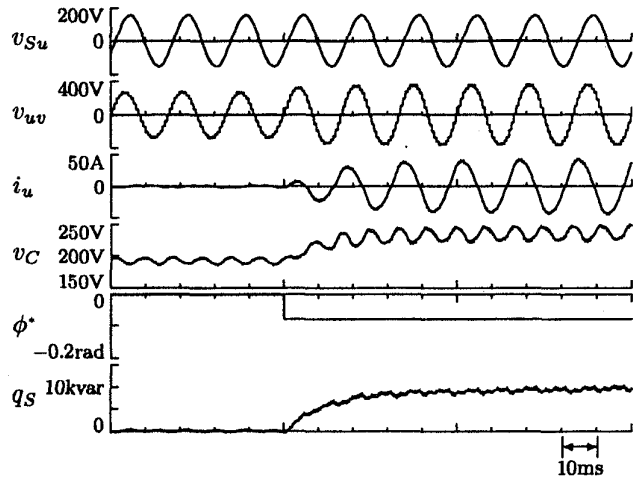
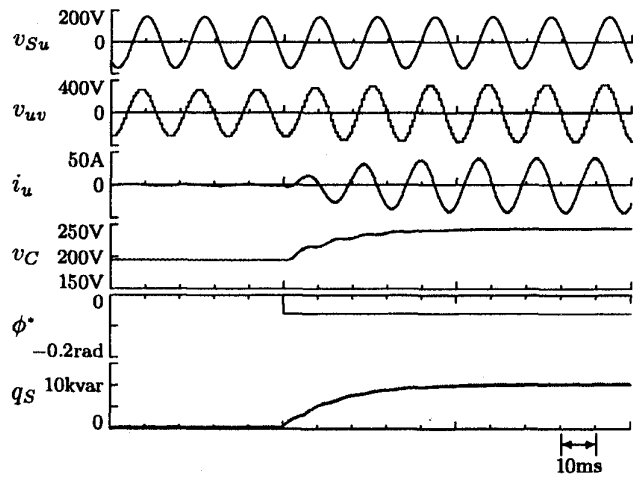Fig. 10. Experimental waveforms for a step change of ϕ, where $C = 500$ μF.

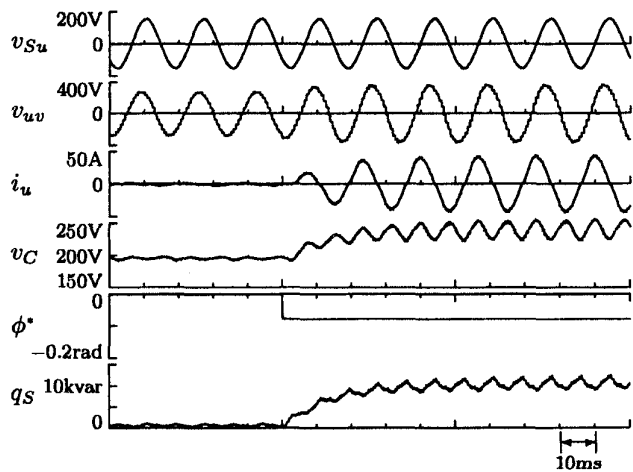Fig. 11. Simulated waveforms for a step change of ϕ, where $C = 1000$ μF.

Fig. 12. Experimental waveforms for a step change of ϕ, where $C = 1000$ μF.

3.5×10^{-5} rad/var and a PI controller time constant T_I of 11 ms, is added to the control circuit. After the step
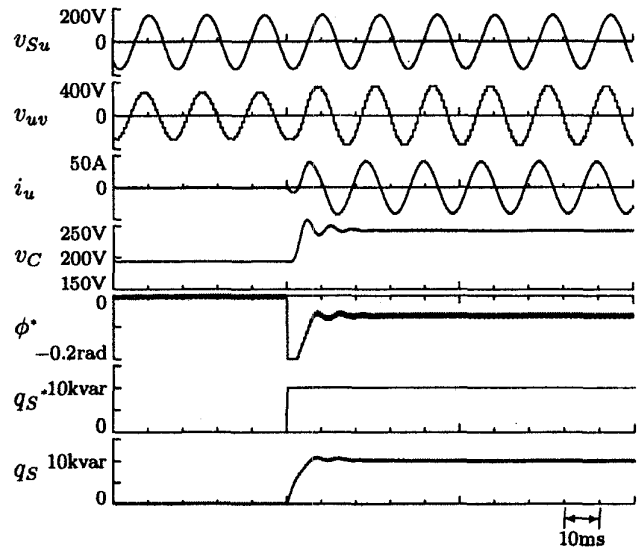

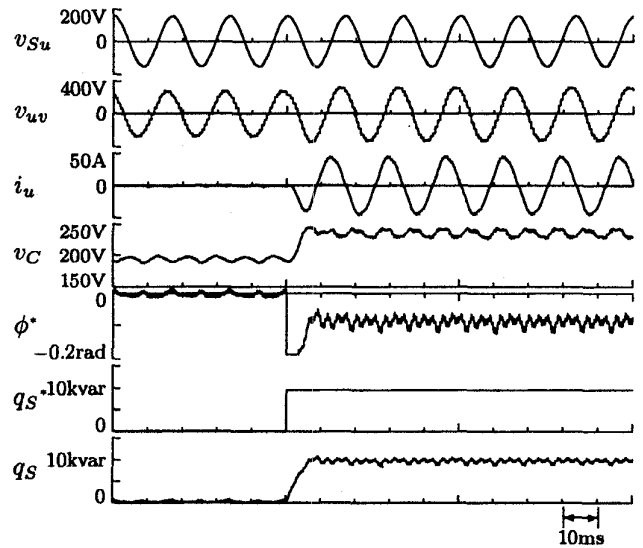Fig. 13. Simulated waveforms for a step change of q_S^*, where $C = 500$ μF.

Fig. 14. Experimental waveforms for a step change of ϕ, where $C = 500$ μF.

change, v_C and q_S reach their final steady-state values in 10 ms. In Figs. 14 and 16, the time constant of the transient response is 5 ms, irrespective of the value of capacitance C. The response time is much faster than the times required in practical applications.

VI. EFFECT OF DC VOLTAGE-REGULATING CONTROL

The effect of the dc voltage-regulating control is discussed as follows. Figs. 17 and 18 show block diagrams of the SVC, without (Fig. 17) and with (Fig. 18) a dc voltage-regulating control loop with a proportional gain K_p, respectively. In Fig. 18, the dc capacitor voltage variation Δv_C is given by
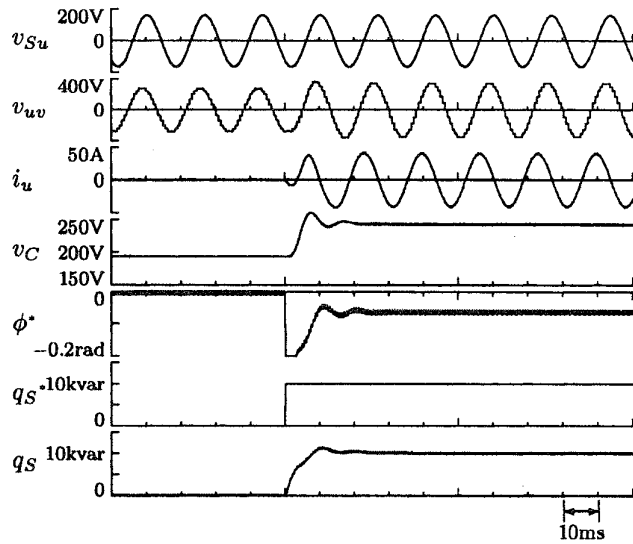
$$\Delta v_C = v_C - v_C(0)$$

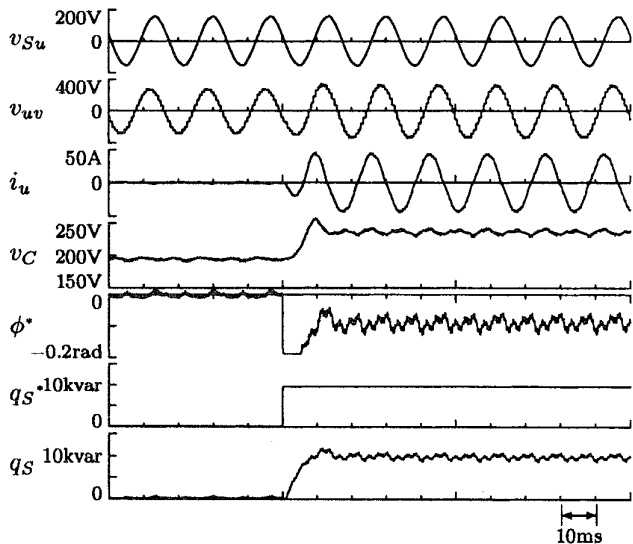Fig. 15. Simulated waveforms for a step change of q_S^*, where $C = 500$ μF.

Fig. 16. Experimental waveforms for a step change of q_S^*, where $C = 1000$ μF.
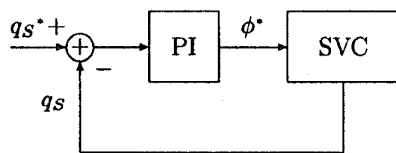

Fig. 17. Block diagram of SVC without dc voltage-regulating control.

where

$$v_C(0) = V_S/K.$$

If $K_p = 0$, Fig. 18 becomes the same as Fig. 17.

Figs. 19 and 20 show simulation results for the same parameters as indicated in Fig. 13 except for the addition of the dc voltage-regulating control loop. A large fluctuation in
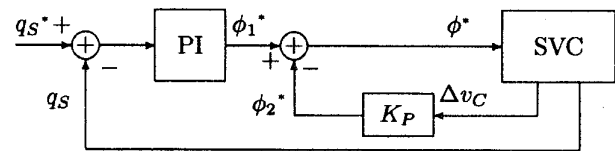

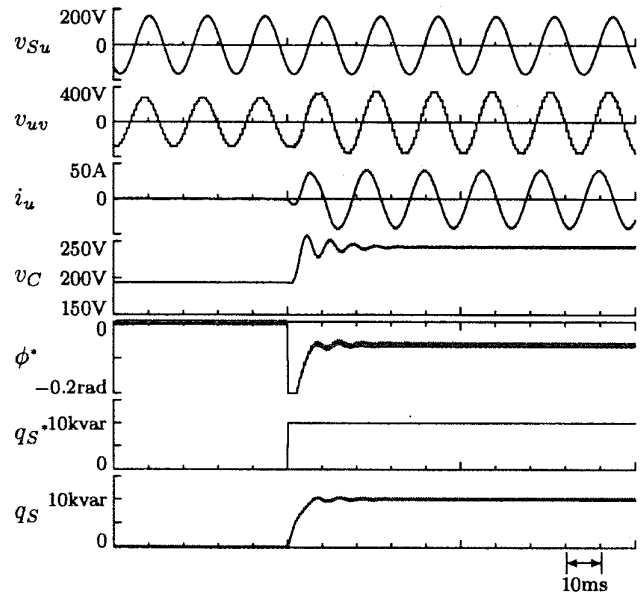Fig. 18. Block diagram of SVC with dc voltage-regulating control.

Fig. 19. Simulated waveforms in the case of adding dc voltage control, where $K_p = -0.6 \times 10^{-3}$ rad/V.

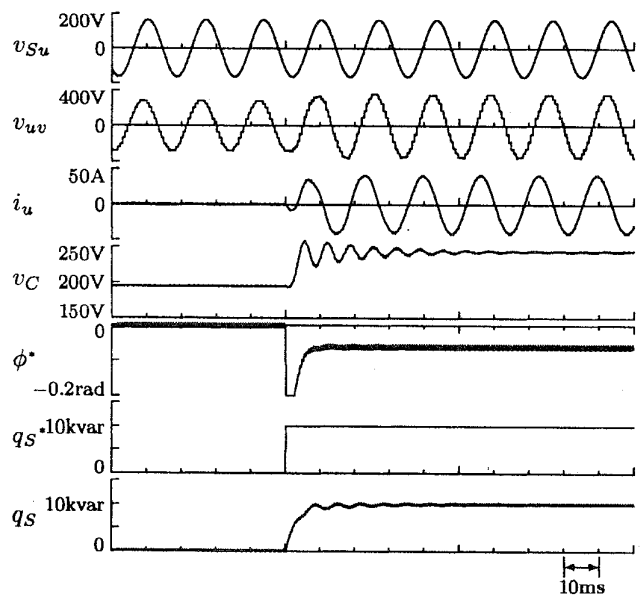Fig. 20. Simulated waveforms in the case of adding dc voltage control, where $K_p = -1.2 \times 10^{-3}$ rad/V.

the dc voltage appears in Figs. 19 and 20, compared with Fig. 13. The dc voltage-regulating control loop has no effect on improving the stability of the dc voltage.

As is well-known, the addition of a current minor loop inside a speed major loop in an adjustable speed drive makes a great contribution to improving torque stability [9]. The reason is that the response time of the minor loop is 5–10 times faster than that of the major loop. However, the dc voltage-controlled SVC has the same response time with respect to i_p, i_q and v_C because (12), (17), and (18) have the same characteristic equation. Thus, the dc voltage minor loop in Fig. 18 does not improve any dc voltage stability.

VII. CONCLUSION

In this paper, the transient analysis of the dc voltage-controlled SVC consisting of quad-series voltage-source non-PWM inverters has been explained in detail. A pq theory-based model for the SVC has been developed to explore the transient behavior caused by changes in power flow between the ac and dc sides. The experimental results obtained from the laboratory system show concurrence with the analytical ones.

The theoretical analysis explored in this paper has clarified the following:

- The time constant of the transient response of reactive power is determined by the equivalent inductance and resistance rather than the capacitance value of the dc capacitor.
- The SVC may exhibit a resonance interaction between the dc capacitor and the ac reactors at a specific frequency.

For the above reasons, the dc capacitor should be designed to avoid the resonance condition rather than to improve the transient response.

Moreover, the feedback control of instantaneous reactive power has made it possible to achieve a response time of 5 ms, which is fast enough to be used in practical applications. The authors believe that the dc voltage-controlled SVC is more suitable for compensating reactive power and/or stabilizing power systems than the pulse-width-modulated SVC.

APPENDIX
TRANSIENT RESPONSE WITHOUT APPROXIMATION

The approximation in (13) can be applied to most typical systems, but not to an SVC which is equipped with a very large capacitor on the dc side. Assuming that $-\alpha$ is a real root of the characteristic equation, (12) can be represented with the use of α as

$$
\begin{aligned}
I_q(s) &= -\frac{1}{(s+\alpha)(s^2+\beta s+\gamma)} \\
&\times \left\{ \frac{\sin\phi}{L}s + \frac{R}{L^2}\sin\phi + \frac{\omega_0}{L}(1-\cos\phi) \right. \\
&\left. + \frac{K^2}{L^2 Cs}\sin\phi\cos\phi \right\} \cdot V_S \\
&= \left(\frac{D_1}{s+\alpha} + \frac{D_2 s + D_3}{s^2+\beta s+\gamma} \right) \cdot \frac{V_S}{s} \\
&= \left(\frac{D_1/\alpha + D_3/\gamma}{s} - \frac{D_1/\alpha}{s+\alpha} \right. \\
&\left. - \frac{(s+\beta)D_3/\gamma - D_2}{s^2+\beta s+\gamma} \right) V_S
\end{aligned}
\tag{19}
$$

where

$$
D_1 = \frac{1}{\alpha^2 - \alpha\beta + \gamma} \left\{ \frac{R\alpha}{L^2}\sin\phi + \frac{\omega_0\alpha}{L}(1-\cos\phi) \right.
$$

$$
\left. -\frac{\alpha^2}{L}\sin\phi - \frac{K^2}{L^2 C}\sin\phi\cos\phi \right\}
$$

$$
D_2 = -\frac{\sin\phi}{L} - D_1
$$

$$
D_3 = -\frac{R}{L^2}\sin\phi - \frac{\omega_0}{L}(1-\cos\phi) + \frac{\alpha}{L}\sin\phi + D_1(\alpha - \beta).
$$

Thus, the reactive power time constant is given by

$$
T = \frac{1}{\alpha}. \tag{20}
$$

The analytical solution of α can be easily obtained by using the equation-solving function in Mathematica (mathematical symbolic computation software). The computation result for α is, however, not shown here because its expression is too complex. The theoretical results indicated by the solid lines in Fig. 5 are numerical solutions.

REFERENCES

[1] H. Akagi, Y. Kanazawa, and A. Nabae, "Instantaneous reactive power compensators comprising switching devices without energy storage components," IEEE Trans. Ind. Applicat., vol. IA-20, pp. 625–630, May/June, 1984.
[2] L. T. Morán, P. D. Ziogas, and G. Joos, "Analysis and design of a three-phase synchronous solid-state var compensator," IEEE Trans. Ind. Applicat., vol. 25, pp. 598–608, July/Aug. 1989.
[3] F. Ichikawa, K. Suzuki, T. Nakajima, S. Irokawa, and T. Kitahara, "Development of self-commutated SVC for power system," in Proc. 1993 PCC, Yokohama, Japan, no. D1-6, pp. 609–614.
[4] K. Suzuki, T. Nakajima, S. Ueda, and Y. Eguchi, "Minimum harmonic PWM control for self-commutated SVC," in Proc. 1993 PCC, Yokohama, Japan, no. D1-7, pp. 615–620.
[5] N. S. Choi, G. C. Cho, and G. H. Cho, "Modeling and analysis of a static var compensator using multilevel voltage source inverter," in Proc. 1993 IAS Annu. Meeting, Toronto, Ont., Canada, pp. 901–908.
[6] L. Gyugyi, "Reactive power generation and control by thyristor circuit," IEEE Trans. Ind. Applicat., vol. IA-15, pp. 521–532, Sept./Oct. 1979.
[7] Y. Sumi, Y. Harumoto, T. Hasegawa, M. Yano, K. Ikeda, and T. Matsura, "New static var control using force-commutated inverters," IEEE Trans. PAS, vol. PAS-100, no. 9, pp. 4216–4223, Sept. 1981.
[8] L. Gyugyi, N. G. Hingorani, P. R. Nannery, and N. Tai, "Advanced static var compensator using gate turn-off thyristors for utility applications," CIGRE, pp. 23–203, 1990 Session.
[9] W. Leonhard, "Control of electrical drives," in Electric Energy Systems and Engineering Series. Berlin: Springer-Verlag, 1985, pp. 67–70.

Hideaki Fujita (M'91) was born in Toyama Prefecture, Japan, on September 10, 1965. He received B.S. and M.S. degrees in electrical engineering from Nagaoka University of Technology, Nagaoka, Japan, in 1988 and 1990, respectively.
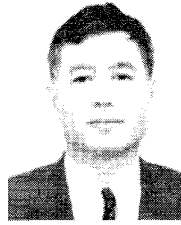
Since 1991, he has been a Research Associate in the Department of Electrical Engineering at Okayama University, Okayama City, Japan. His research interests are static var compensators, active power filters and resonant converters.

Mr. Fujita received two first prize paper awards from the industrial power converter committee of the IEEE Industry Applications Society in 1990 and 1995.
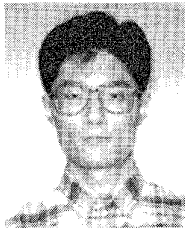
Shinji Tominaga was born in Hyogo Prefecture, Japan, on December 26, 1969. He received B.S. and M.S. degrees in electrical engineering from Okayama University, Okayama City, Japan, in 1993 and 1995, respectively. He is currently enrolled in the Ph.D. program in power electronics at Okayama University.

He is a corecipient of the first prize paper award from the industrial power converter committee in the IEEE Industry Applications Society in 1995.

Hirofumi Akagi (M'87–SM'94–F'96) was born in Okayama City, Japan, on August 19, 1951. He received the B.S. degree from Nagoya Institute of Technology, Nagoya, Japan, in 1974 and M.S. and Ph.D. degrees from the Tokyo Institute of Technology, Tokyo, Japan, in 1976 and 1979, respectively, all in electrical engineering.

In 1979, he joined Nagaoka University of Technology as an Assistant and then Associate Professor in the Department of Electrical Engineering. In 1987, he was a visiting scientist at the Massachusetts Institute of Technology, Cambridge, MA, for ten months. Since 1991, he has been a Professor in the Department of Electrical Engineering at Okayama University. His research interests include power electronic circuits and systems, and their industrial and utility applications.

Dr. Akagi is a corecipient of the first prize paper award in the IEEE TRANSACTIONS ON INDUSTRY APPLICATIONS for 1991 and four IEEE/IAS committee prize paper awards.